Compensation for Shear-wave Anisotropy Effects Above a Heavy Oil Reservoir

Richard Bale*, Kostya Poplavskii and Colin Wright
CGGVeritas, 2200, 715 5th Avenue SW, Calgary, Ab., T2P 5A2.
Richard.Bale@CGGVeritas.com

Summary

Significant shear-wave splitting effects, an indicator of azimuthal anisotropy, have been observed on multicomponent data acquired over a heavy oil reservoir. The orientation of the fast shear wave was initially estimated by visual inspection. A full analysis, using a robust least-squares method, was then performed which confirmed the initial estimates, and provided a spatial map of the orientation and strength of anisotropy. Compensation for the splitting effects produced improved imaging. Independent analysis of shallow well log measurements supported the multicomponent data, with both the log and multicomponent anisotropy orientations differing from assumed regional stress directions.

Introduction

Converted-wave (PS) data from multicomponent seismic surveys are being used to characterize heavy oil reservoirs, with objectives such as mapping density changes associated with shale plugs (Dumitrescu et al., 2003; Gray, 2003), detecting viscosity changes and mapping steam fronts (Watson et al., 2002; Lines et al., 2005). However, a continual challenge with using the PS data is resolution which falls short of the corresponding PP resolution, even after compression to the PP time frame. Among others, one possible cause of resolution loss is the presence of uncorrected, or poorly corrected, shear-wave splitting in the overburden – associated with some form of azimuthal anisotropy. Possible causes are differential stress and the presence of fractures.

Standard PS processing involves rotating to radial (source-receiver) and transverse (orthogonal to radial) coordinates, and then using the radial component to generate the PS image. Shear-wave splitting causes azimuthally dependent time delays of the radial component data which then results in frequency loss when stacked. Uncorrected splitting also implies that useful energy is left on the transverse component rather than being used in the PS image formed from the radial component.

In other contexts, such as carbonate reservoirs or fractured shales, the shear-wave splitting contains useful information on the reservoir, and is analysed for that purpose. However, splitting in the near surface above the target is primarily an impediment to accurate high fidelity imaging.

The data used in this paper displayed strong evidence of shallow shear-wave splitting. This was initially observed using azimuthally sectored stack gathers with super-binnned asymptotic conversion point (ACP) data, at a number of hand selected locations. One such analysis is shown in figure 1. The radial component on the left displays significant variation in arrival times, while the transverse component on the right displays a characteristic change of polarity at 90˚ intervals. By observing the locations of these polarity changes, the fast or slow directions are identified. The ambiguity between fast and slow is resolved by looking at the arrival time of the event on the radial gather. The 130˚ direction indicated is therefore interpreted as a fast (S1) orientation.

More detailed analysis was performed on the complete dataset, using a prestack shear-wave splitting analysis and compensation scheme, which is now briefly described.

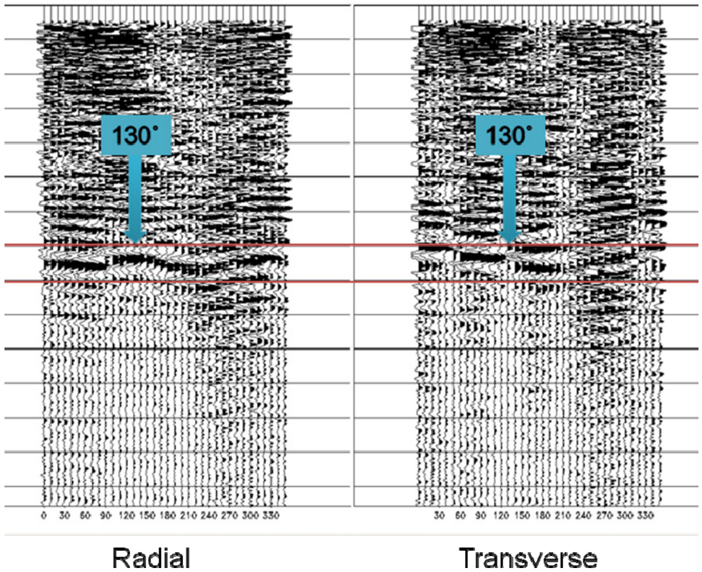

Figure 1. Radial and transverse PS data after azimuthal sector stacks over an 11x11 superbin of asymptotic conversion point gathers. The data are displayed as a function of azimuth from 0˚ to 360˚.

Method

First, a least-squares analysis of the transverse component amplitudes (Bale et al., 2005) is used to ascertain the azimuth of the fast shear direction and the time delay between fast and slow shear waves. The method can be used either on azimuthally stacked data, as shown in figure 1, or directly on prestack gathers.

The gather is then rotated to the S1-S2 coordinate system, and is summed using an optimal stacking method to generate S1 and S2 traces. These traces are correlated to determine the total time delay between S1 and S2 signals. Then a time-variant shift, linearly interpolated between centers of analysis windows, is applied to the slow shear wave to allow recombination of the split waves into a single "isotropized" PS dataset.

The scheme may be applied in a layer stripping fashion to account for changes in the orientation with depth. In this case the center of the previous analysis window serves as the reference time for the time-delay measurement. For the deepest layer analyzed, the results can be output as S1 and S2 oriented data, which may be desirable for amplitude analysis, though this has not been done in the present example.

Results

The method above was applied to data acquired over a heavy oil reservoir – characterized as a mainly clastic overburden above a bitumen sand. The anisotropy estimation was based on analysis at the bottom of the reservoir, where the Devonian provides a strong useable signal. The window used is indicated by the red lines in figure 1. The prestack data were grouped into ACP superbin gathers, with each superbin containing 5x5 original ACP locations. The superbins were fully overlapped.

The analysis provides a spatial map of the orientation and strength of anisotropy, as illustrated in figure 2. The estimated orientations are generally between 90˚ and 180˚. They are somewhat bimodal, with concentrations around 120˚ and 160˚. The delays range from 0 to 40ms, with the mode being approximately 20ms.

Subsequent, independent, analysis of shallow sonic imaging well log measurements for two wells within the 3D supported the multicomponent data to within 10˚-20˚. Interestingly, both the log and multicomponent anisotropy directions were different from assumed regional stress directions, expected to be around 45˚.

Figure 3 shows some of the original analysis gathers generated by azimuthal sector stacking. Figure 4 shows the result of compensating for shear-wave splitting on these gathers. The improvement in alignment of the radial (figure 4a) is evident. Since, the new radial and transverse data are ideally devoid of anisotropy effects, a good QC measure is the amount of residual signal left on the transverse – with ideally no residual signal. In figure 4b, it is apparent that signal has been reduced on the transverse component, though clearly not removed entirely.

In addition to the results shown here, we also performed a two layer analysis – first correcting for splitting above the reservoir, and then estimating splitting in the bitumen layer. On these data, we found that after correcting for the splitting above top reservoir, there was very little residual effect within the bitumen. The time delays in the reservoir were of the order of 0-4ms, compared with 10-20ms delay typical in the overburden. Likewise the estimate of orientation for the bitumen was quite variable, as one would expect for small amounts of measured splitting. On this basis we interpret that the anisotropy is present primarily in the overburden: although, due to the smaller time over which delays are measured for the reservoir layer, important anisotropy there cannot be discounted. In any case, we found that the splitting was most robustly measured by analysis from surface to bottom reservoir, due to the strong signal of the Devonian there.

Conclusions

Significant shear-wave splitting effects, an indicator of azimuthal anisotropy, have been observed on multicomponent data acquired over a heavy oil reservoir, initially observed through visual inspection of azimuth sector stacks. Shear-wave splitting analysis was then performed using a prestack shear-wave splitting analysis and compensation scheme. The results from this analysis were consistent with the initial visual inspection. There are indications of significant anisotropy present in the overburden, with appreciable spatial variability. An attempt to separate the effects into overburden and reservoir anisotropy suggested that very little if any anisotropy was present within the bitumen layer.

Independent analysis of shallow sonic imaging measurements at two wells supported the multicomponent data measurements to within 10˚-20˚. Both the log and multicomponent anisotropy orientations were different from assumed regional stress directions: the factors which give rise to these anomalous near surface anisotropy effects are not yet known, but have also been observed in other heavy oil areas.

Finally, the data after compensation showed significant improvement in alignment of signal on the PS gathers, resulting in an improved image after stack and migration.

Acknowledgements

We thank our anonymous client for permission to show these results, and also Wayne Nowry and his multicomponent processing team for their assistance in processing the data.

Reference

Bale, R. A., Li, J., Mattocks, B., and Ronen, S., 2005, Robust estimation of fracture directions from 3-D converted waves: 75th Annual International Meeting, SEG, Expanded Abstracts, 889–892.

Dumitrescu, C., Gray, D, Bellman, L. and Williams, A., 2003, PS and PP AVO Analysis: A Multi-component Seismic Case Study for the Long Lake Oil Sands Project, CSEG/CSPG Joint Conference Abstracts.

Gray, F.D., 2003, P-S converted-wave AVO: 73rd Annual International Meeting, SEG, Expanded Abstracts, 165-168.

Lines, L., Zou, Y., Zhang, A., Hall, K., Embleton, J., Palmiere, B., Reine, C., Bessette, P., Cary, P. and Secord, D., 2005, Vp/Vs characterization of a heavy-oil reservoir: 75th Annual International Meeting, SEG, Expanded Abstracts, 1397–1400.

Watson, I. A, Lines, L.R. and Brittle, K.F., 2002, Heavy-oil reservoir characterization using elastic wave properties: The Leading Edge, **21**, 736–739.

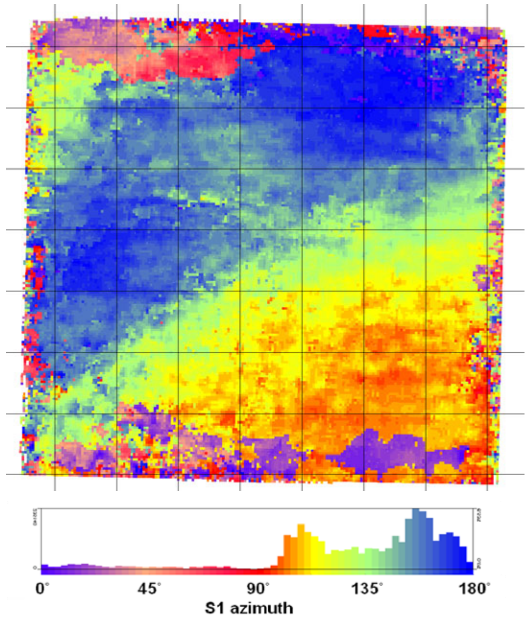

(a)

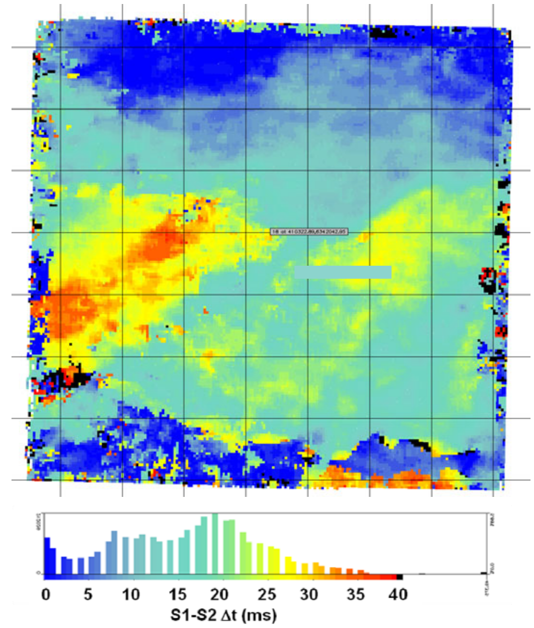

(b)

Figure 2. Results of shear-wave splitting analysis at bottom reservoir horizon: (a) S1 azimuth direction and (b) S1-S2 time delay.

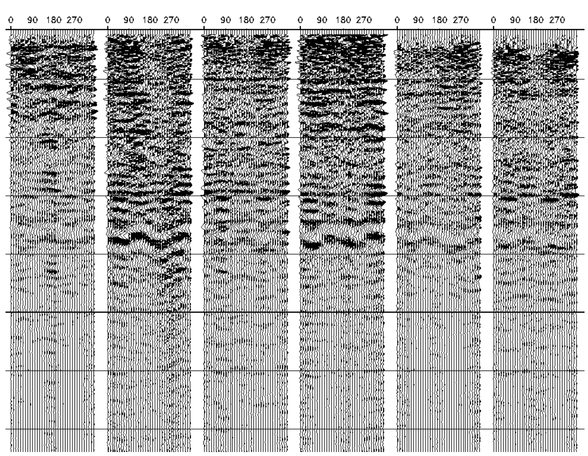

(a)

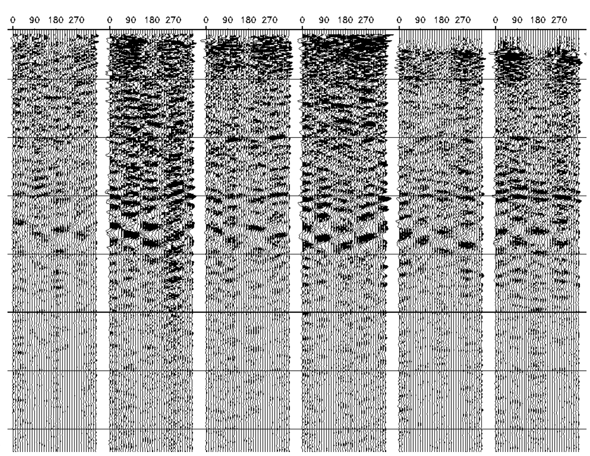

(b)

Figure 3. Azimuthal stack gathers of radial (a) and transverse (b) at selected locations.

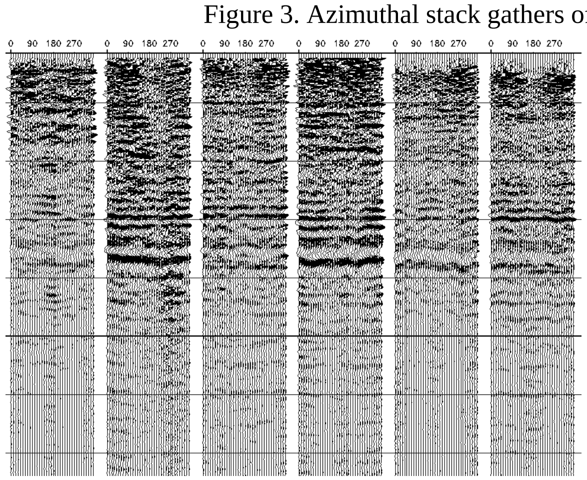

(a)

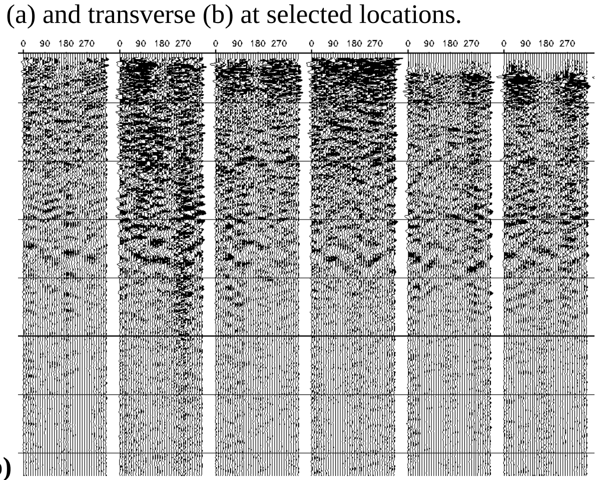

(b)

Figure 4. Date from figure 3 after application of layer stripping. Note improved alignment of signal on radial (a), and reduction of signal on transverse (b).